FUSION OF STEREOGRAMMETRIC AND INSAR DATA FOR ADVANCED TOPOGRAPHIC MODELLING IN ARCTIC DESERTS

Gerhard Brandstätter, Graz University of Technology, Austria
Aleksey I.Sharov, Moscow State University of Geodesy and Cartography, Russia
E-mail: bt@geophot.tu-graz.ac.at and sharov@dib.joanneum.ac.at

ABSTRACT
This paper describes the first stage of a study aiming to evaluate the potential and limitations of stereophotogrammetric and INSAR data for detailed topographic research in arctic deserts. Several different image processing techniques, including digital stereoplotting with Russian spaceborne KATE-200 photographs, photometric segmentation of stereophotographs and ERS-1/2-SAR interferogram differencing, have been tested and practically applied for topographic modelling of several large ice caps in the Franz Josef Land archipelago, Russian High Arctic. The stereophotographic, stereophotometric and interferometric data obtained were merged for the purpose of intercomparative analysis, quality control and methodological developments. Several new methodological variants of image processing have been proposed for the enhanced reconstruction of the ground surface in a relatively flat glacier terrain. The results of relative accuracy analysis are discussed.

1. INTRODUCTION

One-sixth of the land area of the globe, i.e. over 23 million square kilometres belong to the regions of "cold deserts" characterised by perpetual ice and snow cover, intense cold and negligible pioneer vegetation in stony and sandy "oases" during the short summer season. In secluded archipelagos of the European Arctic sector poleward of latitude 75°N, the physiographic zone of arctic deserts occupies nearly 59,000 km², which accounts for about 0.6% of the European "terra firma". This immense inaccessible and inhospitable tract of insular land remains, nowadays, the largest "white spot" in our basic topographic knowledge on the "Old World".

The monotonous landscape of arctic deserts with mostly homogeneous glacial topography, generally uniform land cover and invariably high reflectance properties is subject to rapid changes due to the impact of wind, ice and water, and is regarded as a very problematic object for detailed topographic studies by conventional means (Figure 1). The accuracies of stereophotogrammetric modelling via aerial photographs and/or satellite optical imagery, especially the vertical accuracy of measurements and contouring in extensive glacial areas usually do not meet standard demands (Konecny 1966, 1996). Precise photogrammetric processing of optical imagery is mostly hampered by the high albedo of glacial landscapes, shadows obscuring details, and the lack of reliable ground control. Featureless zones and an almost complete lack of visible contrast render image processing extremely difficult. Often not even visual tiepointing over large polar ice caps and domes can be performed in optical imagery or radar scenes. The automatic procedures of radiometric correlation used for image matching and DEM generation in glacial areas generally yield even more unsatisfactory results since "there is nothing to correlate".

Methods of satellite radar SAR-interferometry (INSAR) provide a new tool to study the detailed topography and environmental changes over prominent ice sheets in the High Arctic. This tool is especially applicable to the detailed topographic study of barren landscapes with a relatively flat topography, and it is generally accepted that the INSAR method is capable of playing a key role in polar remote sensing. It was reported, for example, that a relative elevation accuracy on the order of 2.5 m and an absolute accuracy of about 4 m could be achieved over extensive glacier sheets with ERS-1-SAR repeat-pass interferometry (Joughin et al. 1996). Relevant data on accuracies of polar topographic interferometry, however, are still very sparse and represent rather modest results, which were sometimes achieved without any reliable ground control. The real applicability of this technique for reliable operational topographic modelling in the European High Arctic has yet to be tested in practice in order to be able to define the most efficient way of using INSAR data.

Several recent publications devoted to INSAR topographic applications attest to the expedience of fusion with other image data, preferably from the optical range. To our knowledge the subject of combining INSAR image data with optical stereoimages was first mentioned in a report by the French scientists L.Renouard, F.Perlant and P.Nonin in 1993, who focussed on the generation of digital elevation models (DEMs) in the French Alps. The impact of stereo SPOT and INSAR data fusion on the reliability, completeness and integrity of topographic modelling in the framework of the ORFEAS (Optical-Radar sensor Fusion for Environmental ApplicationS) action has been discussed in (Crosetto & Crippa 1998). By merging SAR and multispectral image data the accuracy of land use classification can be significantly improved (Hellwich 1999). Experiments in the past have shown the combined use of stereographic and microwave data to be very expedient for advanced topographic modelling in mountainous and hilly areas with significant slopes, where the radar imagery is subject to layover, shadowing and other topographic effects (Small et al. 1996).

While other studies used stereogrammetric and interferometric data fusion in order to improve the results of topographic interpretation and to complete obscured areas, we applied this approach mostly to methodological tests, accuracy control and the determination of general relations between stereogrammetric and interferometric methods of image analysis. In contrast to previous investigations we concentrated on merging stereographic and interferometric data for the enhanced reconstruction of the ground surface in relatively flat terrain. Several different techniques, including

- digital stereoplotting with Russian aerial and spaceborne KATE-200 photographs;
- stereophotoclinometry, a new technique based on photometric segmentation for image processing under low optical contrast;
- ERS-1/2-SAR interferogram differencing

were practically applied to the detailed topographic modelling of several large ice caps in the Franz Josef Land archipelago (FJL), Russian High Arctic. Several original methodological variants of data fusion were specially designed to ensure the combination and comparison of the resultant data sets with one another and with available ground control data.

2. DATA PREPARATION

Four spaceborne stereophotographs obtained at an original scale of 1:1,250,000 by a KATE-200 film camera (1st spectral channel, 635-690 nm, photogrammetric focal length of 201.342 mm), 9 complex ERS-1/2-SAR images constituting 5 INSAR image pairs, and 8 old aerial photographs taken over the same territory were collected for basic experimental investigations (Table 1). Besides, several high-resolution spaceborne stereoscopic photographs acquired over FJL by RESOURCE-F1, KFA-1000 and CORONA, KH-4(A) systems as well as 2 precision ERS-1 radar scenes were used for the identification of ground control and check points. All necessary cartographic materials and ground-truth data were also available.

Figure 1. Typical glacial landscape in the High Arctic, Russkiy Ice Cap, Franz Josef Land

To provide high-resolution, high-quality digital image input for computer-based processing the analog image set was digitised at the VEXCEL3000 Image Scanning System with a maximum attainable spatial resolution of 1,250 and 2,500 dots per inch (DPI) so that pixel sizes were 20 and 10 microns, respectively. The spatial resolution of digitised images was principally chosen to avoid any geometric loss and to ensure that the digital imagery used for joint analysis is of similar scale, resolution and size. For instance, KATE-200 photographs from the first spectral band digitised with a spatial resolution of 1,250 DPI offer a ground resolution of about 25 meters, which is similar to that of ERS-1/2-SAR imagery. Thus, comparable detailedness of image input can be achieved. Several old aerial photographs were scanned with a spatial resolution of 300 and 600 DPI in order to perform comparative accuracy tests. Practical image processing was performed using the ADOBE Ph.5.0, ENVI 3.0, PHOTOMOD 1.6 and RSG 3.21 software packages.

In order to reduce the processing time, we did not digitise the entire imagery, but only the fragments corresponding to the test sites. In our case the most interesting test sites with different types of glacial cover and some ice-free areas comprise three large islands, namely Ziegler Island with a total land area of 404.0 km² and a maximum elevation of 554 m a.s.l., Becker Island (37.5 km² and 165 m) and Kane Island (23.5 km² and 282 m). In total, 6 digital fragments from KATE-200 imagery and 8 fragments from aerial photographs were prepared. The largest fragment depicting Ziegler Island with surrounding areas in the central part of FJL covers an area of 37 x 44 square kilometres.

2. DIGITAL STEREOPLOTTING WITH KATE-200 PHOTOGRAPHS

KATE-200 stereoscopic image fragments served as a basis for photogrammetric precision modelling and complete three-dimensional vectorisation of the topography in test areas, including consistent contouring at 1:100,000 scale. For the major part of the study region a contour interval of 50 meters was chosen for solid contours, which should not be smaller than about three to five times the rms (root mean square error) height accuracy (Leberl 1989). The highest elevation in the region is 554 meters, which means that a total of 12 contour layers, including the shoreline, had to be vectorised.

Contouring in homogeneous glacial areas combined with local topographic interpretation did not bring about the difficulties we had expected and actually was even more convenient than contouring in rocky areas affected by shadows. However, it was very complicated and often impossible to perform contouring in relatively flat and homogeneous terrain at the top of the largest ice domes, which are characterised by very high visible albedo and little image contrast. Nevertheless, the local interpretation of KATE-200, KFA-1000 and CORONA images allowed the precise location of the 27 highest positions within the accumulation area of the glacier to be determined. Their photogrammetric elevations were defined with respect to the current sea level. Due to the manual drawing mode contouring was a relatively time-consuming process and took several weeks, including preparations and corrections.

A satellite basic contour map of Ziegler Island with surrounding areas was printed in six colours at 1:100,000 scale in conformal Gauss projection, which is the usual scale for Russian topographic maps. Contour lines representing elevations of 200 and 400 meters were rendered in darker colours and depression contours were marked by dashes. The elevations given were compiled photogrammetrically with respect to the current level of the Barents Sea. It should be noted that the mean effect of tidal forces in FJL does not exceed 20 to 30 cm and can thus be neglected. Different kinds of shorelines are presented: ice-free and icy shores, precipitous and sloping, steady and changing banks. A small-size black and white copy of this map is given in Figure 2.

Table 1. Description of available remote sensing data

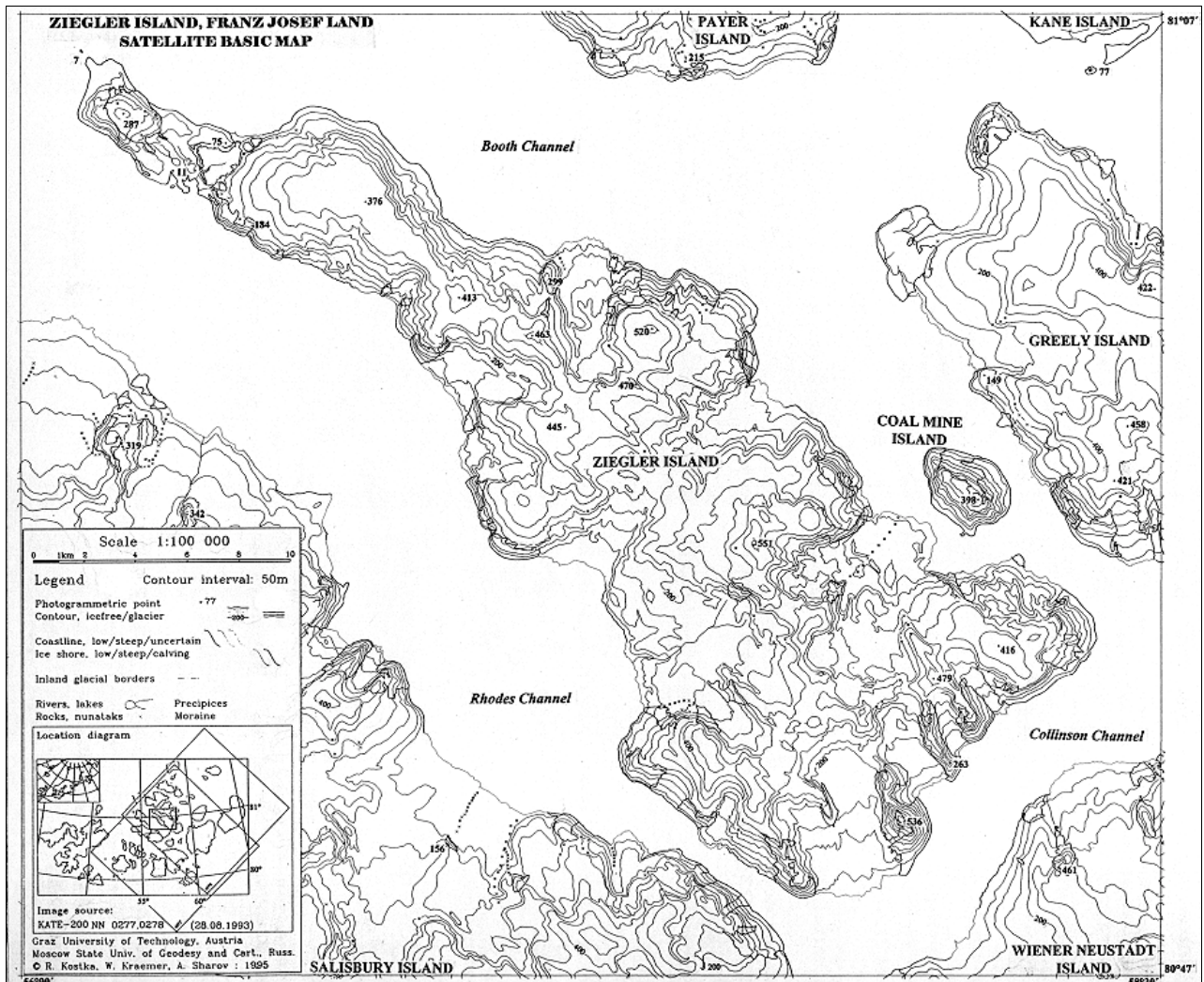| System	Image type, frame No.	Date/time of survey GMT	Base, m/resolution, m	Quantity
KATE-200	Multispectral stereoph. (B), 0218, 0219, 0277, 0278	28.08.93, 07.09.93/ 10:25	90,000 / 18.8 – 24	4
ERS-1/2-SAR	SLC, PRI* 1935, 1953	28.08.93 / 09:20 3/4.09.95, 8/9.10.95 /09:11	49 - 245 / 40 - /25 – 30*	9 2*
AFA-TE100	Stereoph. 5950-53, 4754-57	08.05.53, 21.08.53	2,000 / 0.7 (5 digit.)	8

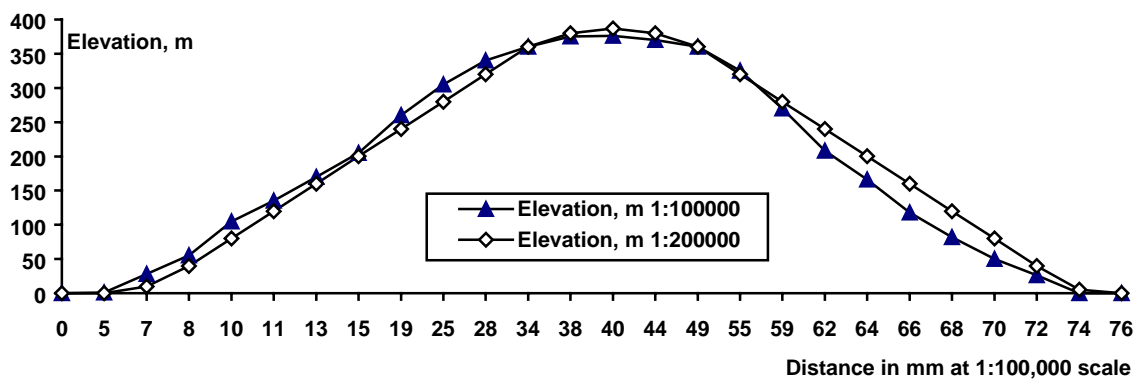Figure 2. Result of stereoplotting with KATE-200 images at 1:100,000 original scale

Figure 3. Transverse profiles across the ice cap derived from traditional and satellite map

Table 1. Results of vertical accuracy test

Control method	Mean difference, m	RMS, m
Check points (27)	- 1.30	± 15.5
Check profiles (3)	- 4.23	± 17.1

The vertical accuracy of the contour base map of Ziegler Island was checked by comparing 27 elevations determined photogrammetrically with respect to the current sea level with those given in available topographic maps at 1:100,000 and 1:200,000 scales in relation to the multiyear mean sea level. Several control elevations related to the multiyear mean sea level were derived from the catalogue of geodetic and navigation spots. The root mean square difference between photogrammetrically derived spot elevations and those given in available cartographic documents did not exceed 15.5 meters. The results of the vertical accuracy test are given in Table 1. The horizontal accuracy of the map was estimated at $\pm$ 25 m rms.

Moreover, contours and spot elevations were checked by means of the profile method, which is based on comparing profiles established in available and newly produced maps directly across the largest ice cap on Ziegler Island. Two of the profiles compared are given in the next graph. The comparison between the profile derived from the available 1:200,000 map with a contour interval of 40 meters and the one established in the satellite map with a 50 m contour interval shows significant elevation differences of several tens of meters, in particular on the right side of the graph corresponding to the northern slope of the ice cap. Apart from the inaccuracies of stereoplotting, which increase in areas affected by shadows (as can be seen on the right side of the graph), some elevation differences might be caused by glacial changes. The mean difference between the compared contour values is given as - 4.23 m and the rms difference is $\pm$ 17.1 m.

Generally speaking, the values obtained are well within the accuracy standard and even surpass theoretically expected accuracies. However, at a very gentle slope of about 1°, which is typical of the majority of glacier tops in the FJL archipelago, the vertical inaccuracy of 17 meters will result in a contour line horizontally displaced from the true position by about 980 meters. No intermediate contours, e.g. at a contour interval of 25 m, could be traced additionally for better height reproduction in these low-contrast areas. Therefore, relatively large tracts of ice at glacier tops up to 10 km² in size were not traced at all. Thus, neither accuracy nor completeness of topographic modelling at homogeneous glacier tops could meet the standard requirements for precise DEM generation. One

possible solution to this problem is given in the next section.

3. PHOTOMETRIC SEGMENTATION – A SUBSIDIARY TOOL FOR GLACIER SURFACE MODELLING

Due to the limited capabilities of human vision, subtle differences in image brightness cannot be directly perceived in homogeneous areas at glacier tops. These variations, depending on the surface topography, land cover, illumination and viewing geometry, usually exist and can be detected if the image is not affected by sensor oversaturation. Under some assumptions we may suggest that, in homogeneous areas with uniform albedo, a line connecting the image points of equal brightness "belongs" to the glacier surface. Thus, a set of such isolines could additionally facilitate the reliable representation of the surface.

The desired set of isolines can be effectively produced by means of photometric segmentation of optical images. The simplest equidistant segmentation consists in converting an original grey scale image to an indexed-colour image with a limited number of grey levels (fewer than 256). The resultant "stepped" image is composed of areas of constant brightness and characterised by the steady brightness difference between adjacent areas. The procedure of high-pass filtering transforms such an indexed-colour image into a system of isolines.

By manipulating the pixel depth of an original image between 3 to 8 bits/pixel the rate of isolines can be varied while maintaining the visual quality required. Greater pixel depth means a higher rate of isolines and a smaller brightness difference between neighbouring lines. Figure 4, a) illustrates the result of photometric segmentation of a KATE-200 image fragment (4 bits/pixel) and, in contrast to Figure 2, shows a number of new elements at the top of an ice cap. Isolines can be hardly detected in ice-free and shadowed areas.

The preeminent orientation of isolines in Figure 4, a) is perpendicular to the along-sun direction marked by the **V** symbol, and it can be seen that the density of isolines per unit area increases at larger slopes. The rate of isolines on the direct (illuminated) slope of an ice cap is lower than on the opposite side. In our case the camera movement nearly coincided with the along-sun direction and the isolines drawn on the KATE-200 image pair can be observed stereoscopically. The stereoscopic

viewing of isolines is distorted in the areas with inhomogeneous albedo, such as areas of wet snow, blue and superimposed ice, crevasses etc.

K.M.Lee and C.J.Kuo, who investigated the stereophotometric approach to the reconstruction of the simplest shapes and the shape-from-shading method, showed that the image brightness in a photometric ratio between two images of the same object is only a function of the surface normal (Lee & Kuo 1996). We suppose that the same holds for the stereophotographic surveying of ice caps in FJL and that the photometric ratio between two stereoscopic KATE-200 images may be

successfully used for the correct and consistent representation of the glacier surface in areas with gentle slopes. That is why the isolines determined in the photometric ratio image were called *isoclinals*. Of course, isoclinals are not contour lines and cannot be directly incorporated into a DEM. In order to verify the correspondence between the isolines obtained by traditional stereoplotting and those resulting from our new approach, the set of isolines derived by segmentation of the photometric ratio was directly merged with the contour plot shown in Figure 2. The result of fusion is shown in Figure 4, b.
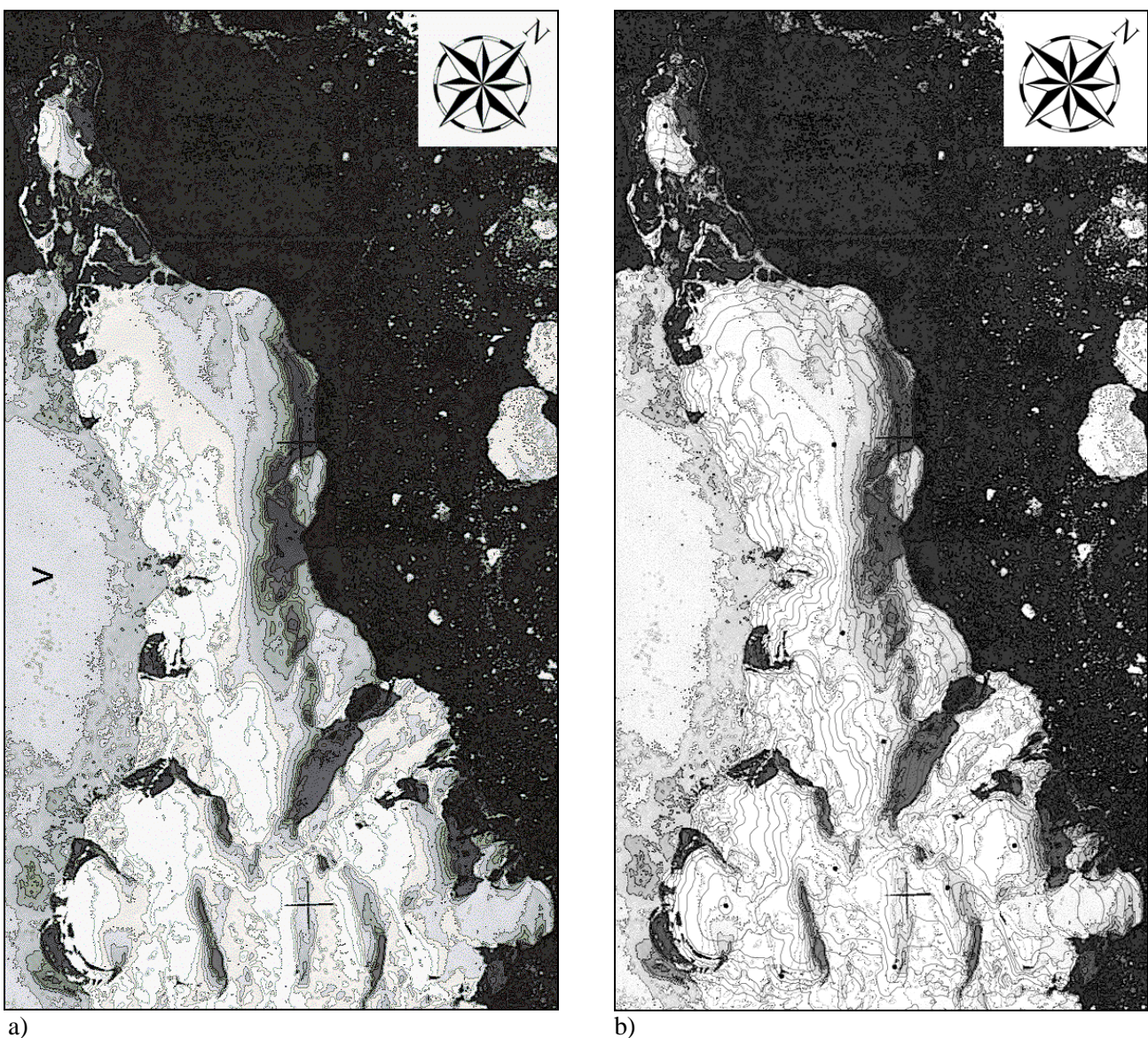
a)   b)

Figure 4. The result of photometric segmentation of KATE-200 image (a);
fusion of a) with the contour plot (b).

The combination shows very good correspondence between data sets, which can be seen very well along the ice divide of the glacier. The conformity in position of the contour plot with photometric features was verified by means of 10 checkpoints. The rms error in the plotted position of checkpoints (marked by •) with respect to the "central" (highest) isocline was evaluated as being less than ± 34 m, which corresponds to a relative height error of less than 1 meter. We assume that our new approach based on automatic procedures of photometric image analysis is capable of providing higher accuracy than traditional stereoplotting in glacial areas. However, further investigations are required to verify the absolute accuracy of stereophotometric modelling and define the basic principles and limitations of the new method called *stereophotoclinometry*. The concept of *optical flow*, i.e. changes of object brightness in successive images due to camera movement (Horn 1989), and related topics could provide valuable information essential to understanding the problem.

There is a very interesting methodological variant of photometric segmentation, which should also be studied in detail. It is based on the use of dithering functions for the representation of the indexed-colour image with a reduced number of colours. Dithering mixes the pixels of the available grey levels to simulate the missing shades of grey. If the diffusion dithering function is applied, the high-pass filtering of the indexed-colour image results in a fringe pattern, which can be considered as a *quasi-interferogram* showing some valuable properties essential to real interferograms. The fringe rate in the optical fringe pattern can be easily changed as explained above. However, increasing the fringe rate decreases the visibility of fringes. Optical fringe patterns for Suvorov Ice Cap on Becker Island and the northeastern part of Ziegler Island (ice caps Nos. 26, 27, 28) are shown in Figures 5, c) and 7, b), respectively.

Such a product allows for a more reliable interpretation of different glacial zones, including the belt of superimposed ice and slush areas, ice divides and ice shores. Certain elements of glacial topography also look more prominent in the fringe pattern. For example, a small river in the left part of the ice cap, as shown in the topographic map (Figure 5, d), is well detectable in the fringe pattern, but could not be reliably detected in optical (Figure 5, a) or radar imagery (Figure 5, b). Besides, the practical implementation of such an approach provides certain evidence on the similarity between the stereophotogrammetric, stereophotometric and interferometric method of image analysis, which means that some stratagems used in radar interferometry, e.g. interferogram differencing, could be applied to streophotographic image processing.
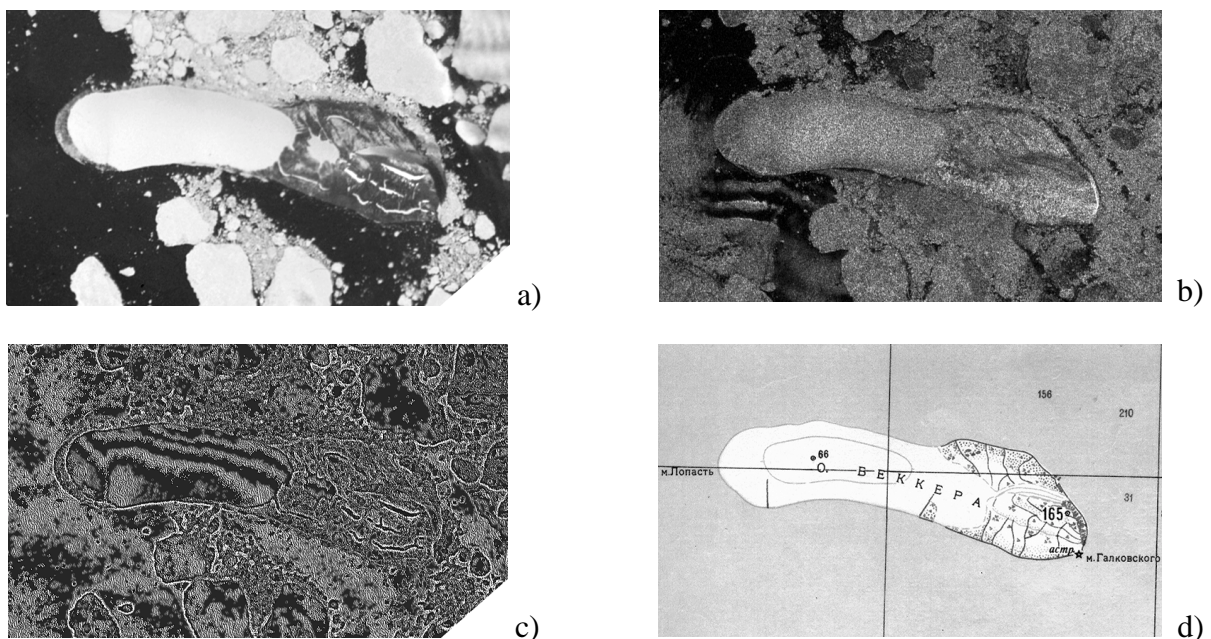

a)

b)

c)

d)

Figure 5. Suvorov Ice Cap, Becker Island on KATE-200 image (a), precision ERS-1-SAR image (b), optical fringe pattern (c), Russian topographic map at 1:200,000 scale (d).

4. INSAR DATA PROCESSING

Previous studies using interferometric ERS-1/2-SAR image data were recently carried out with the aim to further increase the correctness, detailedness and consistency of topographic modelling in the FJL archipelago (Brandstaetter & Sharov 1998). Main emphasis has been put on the differential approach to repeat-pass INSAR data processing based on linear combination of the two original interferograms generated from different SAR image pairs of the same area.

The basic principle of differential interferometry states that the proper linear combination of original interferograms results in a new secondary interferogram. In the resultant interferogram, the width and rate of fringes depends on the value of the virtual (equivalent) baseline B_v, which in turn depends on the kind of mathematical operation applied to the combination of original interferograms. The combination can be done so that the height interval corresponding to one interferometric fringe will exceed the maximum elevation in a region. Then the number of fringes enclosed between the lowest and the highest points in the area will be smaller than one and larger than zero. In a "single fringe interferogram", the interferometric phase can be unambiguously related to topographic height on a pixel-by-pixel basis. Since the single-fringe interferogram provides a more or less realistic view of the terrain, it is sometimes reffered to as *topogram*.

The practical generation of a single-fringe interferogram can be accomplished either by combining two original interferograms with different baselines or by differentiating between the primary interferogram and a *phase filter*, i.e. simulated interferogram with straight fringes being perpendicular to the range direction. Several variants of linear combinations between ERS-1/2-SAR interferograms are illustrated in Figure 6.

a)

b)

$B_2 \cong 130\ m$ $\qquad$ $B_1 \cong -53\ m$ $\qquad$ $B_1 \cong -53\ m$ $\qquad$ $B_v \cong 25\ m$
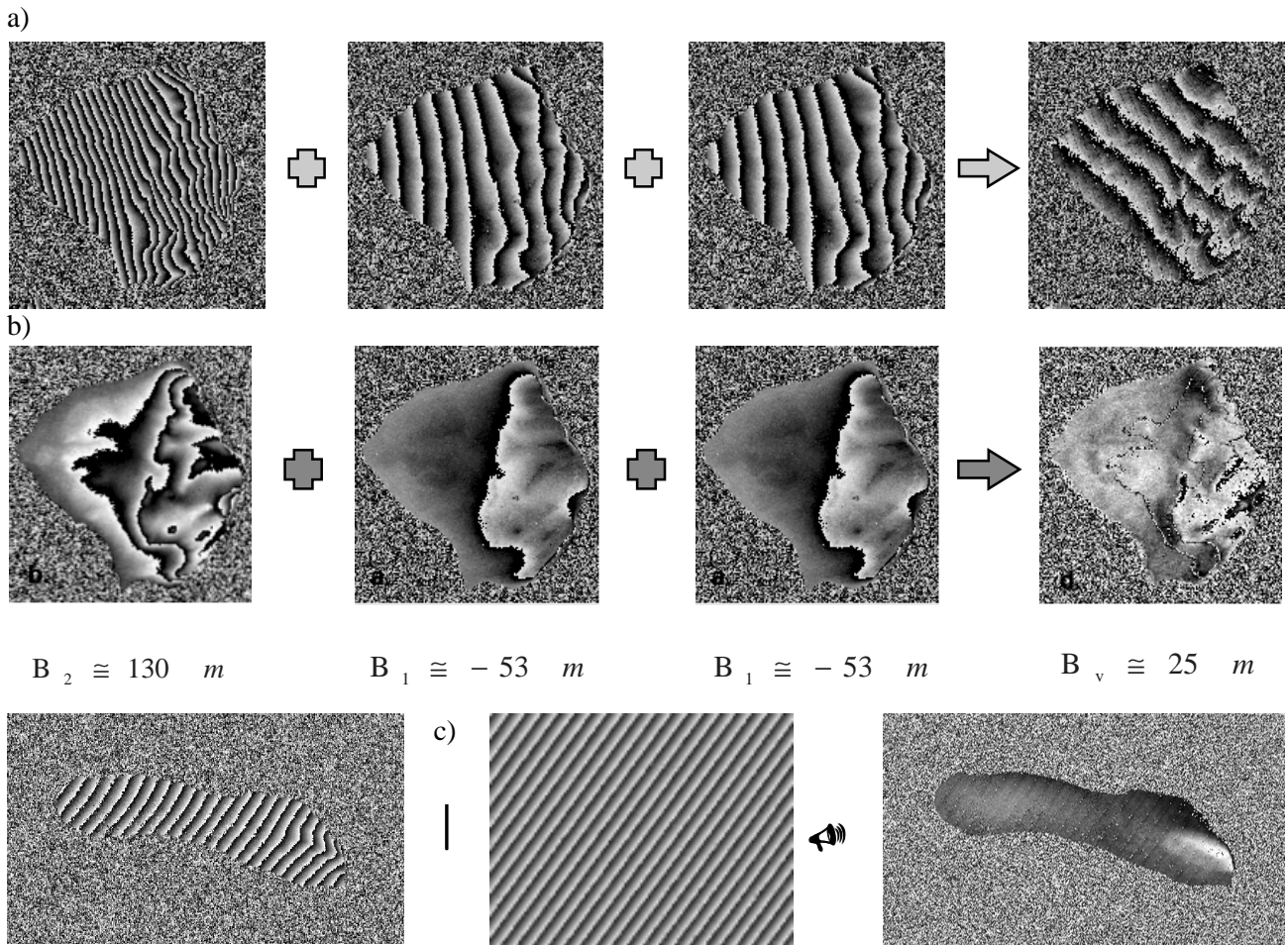
c)

Figure 6. Linear combinations: between two original interferograms of Kane Island (a), between two interferograms of Kane Island after FTP correction (b), between one original interferogram of Becker Island and a phase filter (c).

The linear combination of interferograms may be performed either before (Figure 6, a) or after (Figure 6, b) the "flat terrain phase" correction is performed. The combinatorial approach is based on the co-registration of interferograms, which must be done with sub-pixel accuracy. However, the direct correlation of wrapped fringe patterns is usually impossible, which is why the corresponding coherency images with the same geometry were used to derive the parameters of co-registration. Besides, due to the contradiction between the desirable spatial and temporal baselines, the fine adjustment of the virtual baseline is not always possible.

The approach based on the use of a phase filter usually does not result in such complications and provides a more flexible solution to the phase unwrapping problem. The approximate width of fringes in the phase filter can be derived from the equations given in (Brandstaetter & Sharov 1999). The fine adjustment of the filter can be performed iteratively by changing the filter scale. The additional difficulties brought about by narrow "traces" from the edges of fringes, which can be seen in our topograms (Figure 6, b, c), are, however, more prominent, if a phase filter with a higher rate of fringes is applied.

Besides, it is to be noted that in some cases we were not able to perform full phase unwrapping for high islands. While phase unwrapping of the fringe image was possible in the relatively low areas, this was not always the case in the glacier terrain with rather steep slopes. In available interferograms, the critical elevation corresponds to a height of about 300 meters a.s.l. Nevertheless, the highest positions of several of the largest ice caps, including seven glacier tops at Ziegler Island, were defined and compared with those given in the KATE-200 stereophotographic plot. The highest positions on ice caps were recognized by detecting extreme pixel values in the fringe image in the vicinity of the presumed summit.

5. MERGING STEREOGRAMMETRIC AND INTERFEROMETRIC DATA

Interesting results were obtained by merging interferometric imagery with the graphic layer obtained by stereoplotting from KATE-200 photographs. The rectified KATE-200 digital image has a ground pixel size of 25 meters, and ERS-1/2-INSAR image data acquired over the same area

could be registered to the optical image, since they have similar ground resolutions. However, direct fusion of these heterogeneous image data did not produce the desired results. Significant difficulties were brought about by the different appearance of slant-range INSAR scenes and optical images with different geometry.

Since the transformation of the graphic layer requires much less computing time, it was decided to combine graphical elements with the ERS-1/2-INSAR imagery by transforming the graphic layer itself. In order to fit the fringe image shown in Figure 7, all features in the graphic layer, including 7 checkpoints situated at glacier tops, were shifted layer-by-layer towards the subsatellite track. The shift value can be calculated from the formula

$$D' = h \cdot (\cos\theta - \sin\theta \cdot \tan\frac{\alpha}{2}), \qquad (1)$$

in which the angle α' can be approximately derived as

$$\alpha' \cong 0.5 \cdot \frac{h}{H} \cdot \sin 2\theta, \qquad (2)$$

where h denotes the object elevation; H is the satellite altitude and θ is the local incidence angle.

Prior to superimposition, the graphic plot was appropriately scaled and rotated to fit the shoreline in the fringe image. In Figure 7, the transposed positions of checkpoints are given as ■, and the highest positions in the fringe image are marked with ⓘ.

The comparison between the positions of the transposed checkpoints and the corresponding highest positions identified in the fringe image clearly showed significant positional differences both in range and azimuth direction. The results of measurements show the equal sign of differences at all checkpoints.

The differences in azimuth direction were nearly half as large as those detected in the range direction. In range direction, the differences vary between 100 and 380 meters, which is equivalent to a relative change in vertical position of about 1.7 to 6.6 m on the glacier slope of 1°. The mean difference in vertical position was estimated at 2.8 m.

At the glacier top, the slope influence can be neglected, and, apart from the image processing imperfections, the varying penetration of the radar signal into the dry snow might be a reasonable

explanation for those differences. At the time of investigation, however, we had no ready mechanism reliably explaining the penetration of radar signal into the dry snow, scattering within the snow pack and backscattering from the internal ice layers. Besides, the environmental changes that occurred on Ziegler Island during the period of August 1993 – October 1995 should not be underestimated.

6. CONCLUSIONS

Thus, our research has to be continued in order to determine and investigate all other factors affecting topographic image processing in the High Arctic, e.g. glacier flow, eolean transport of snow, melting, hoar frost etc. The topographic interpretation of INSAR image data taken over extensive glacial areas is very expedient with the aid of stereogrammetric data, which provide additional and complementary information. In this context, our new stereophotometric approach provides a valuable tool for further methodological tests and developments in the field of interferometric image analysis.

7. ACKNOWLEDGEMENTS

8. REFERENCES

Brandstätter G., Sharov A.I., 1998. Environmental monitoring in the High Arctic using different types of high-resolution satellite imagery. IAPRS, v.32, Part 7, 201-210.

Brandstätter G., Sharov A.I., 1999. Metric relations in INSAR topographic modelling. Proc. of the 19-th EARSeL Symp. Balkema, 9 p. (in print).
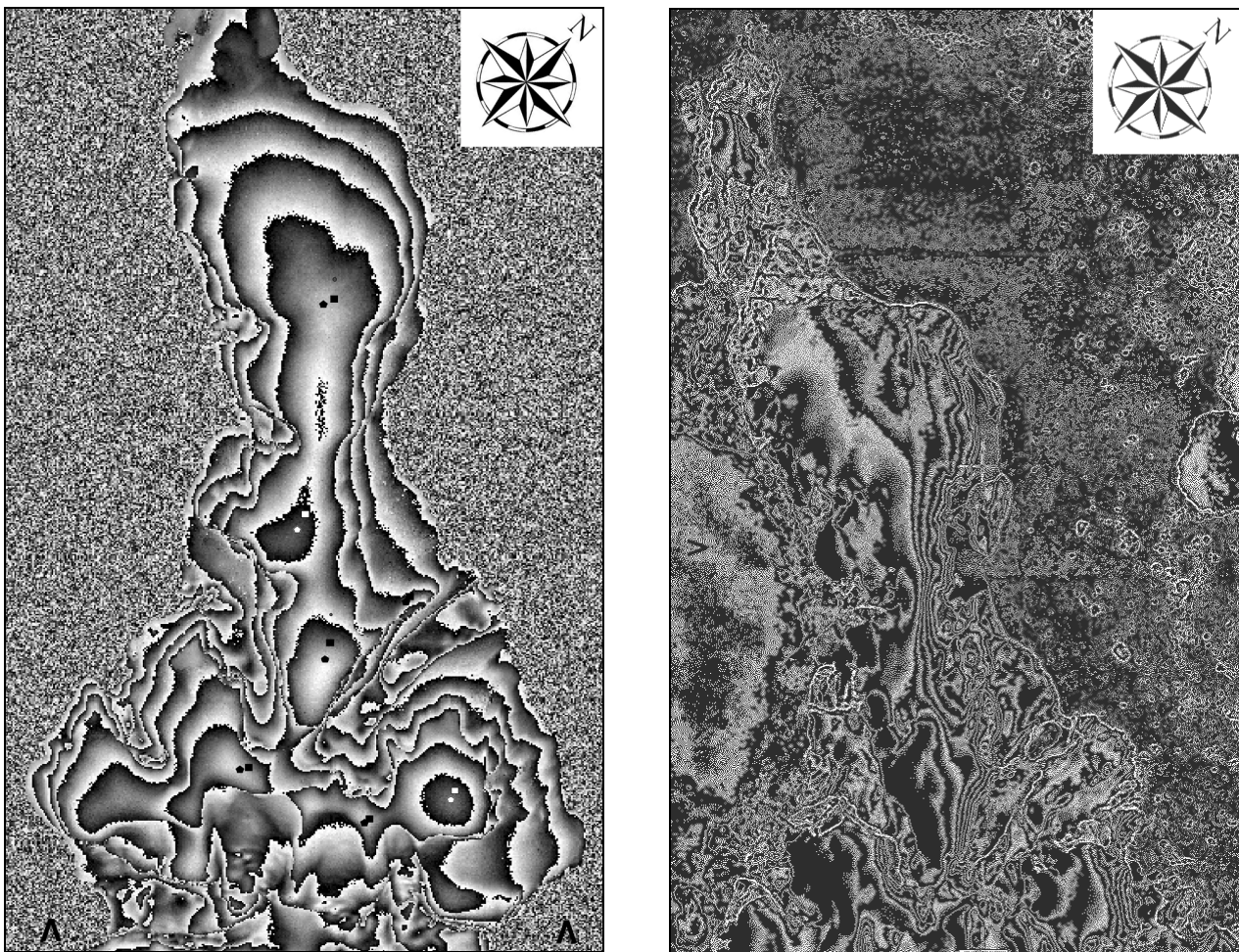

Figure 7. Fringe images of the northeastern part of Ziegler Island: INSAR fringe image with the location of checkpoints given as ■ (a), optical fringe pattern (b); the direction of illumination is marked with Λ.

Crosetto M., Crippa B., 1998. Optical and radar data fusion for DEM generation. IAPRS, v.32, Part 4, pp.128-134.

Hellwich O., 1999. An alternative paradigm for data evaluation in remote sensing using multisensor data fusion. Proc. of the IGARSS'99 Symposium, 3 p. (in print).

Horn B., 1989. Robot vision. Moscow, Mir,488 p.(in Russ).

Joughin I., Winebrenner D., Fahnestock M.,1996. Measurement of ice-sheet topography using satellite-radar interferometry. *J. of Glac.*, v.42, No.140, 11-21.

Konecny G., 1966. Applications of Photogrammetry to Surveys of Glaciers in Canada and Alaska. Canadian J. of Earth Sciences, v.3, No.6, p.783-798.

Konecny G.,1996.Hochauflösende Fernerkundungssensoren für kartographische Anwendungen in Entwicklungsländern. Photogrammetrie und Fernerkundung, Heft 2, p.39-51.

Leberl F., 1989 Radargrammetric image processing. Artech House, L.-A., 595 p.

Lee K.M., Kuo C.J., 1996. Shape from photometric ratio and stereo. J. of Visual Communication and Image Representation, 7(2), p.155-162.

Small D. et al., 1996. ERS-1/2 tandem mission. FRINGE Report to ESA, ESRIN, 11 p.